

# PERFORMANCE OF A BASE-ISOLATED RC BUILDING SUPPORTED ON SQUARE UN-BONDED FIBER REINFORCED ELASTOMERIC ISOLATOR UNDER EARTHQUAKES

*Van-Thuyet Ngo*

Civil Engineering Department, Thuyloi University, Hanoi, VIETNAM

**Abstract:** Un-bonded fiber reinforced elastomeric isolator (U-FREI) is a relatively new type of multi-layer elastomeric isolator in which fiber layers are used as reinforcement to replace steel sheets in conventional steel reinforced elastomeric isolators. It is installed directly between the substructure and superstructure without any connection at the interfaces. Most of the previous studies on the U-FREIs supported to the base-isolated buildings are masonry or stone structures. In this study, the dynamic responses of a reinforced concrete (RC) building supported on square U-FREIs under the action of recorded real time-history ground motions of earthquakes are investigated by finite element analysis using SAP2000 software. A hypothetical 4-storey reinforced concrete building constructed in Vietnam is selected for the study. Comparison of the dynamic responses of the base-isolated building and corresponding fixed-base building is carried out to evaluate the seismic vulnerability of the base-isolated building under earthquakes. Finite element analysis results show that peak values of floor acceleration and inter-storey drifts at different floor levels, and peak value of base shear of the base-isolated building are lower than those of the corresponding fixed-base building. The U-FREIs are found to be very effective in reducing seismic vulnerability of low and mid-rise RC buildings.

**Keywords:** Base isolation, un-bonded fiber reinforced elastomeric isolator, effective horizontal stiffness, effectiveness of base-isolated building, earthquake

# ЭФФЕКТИВНОСТЬ КВАДРАТНОГО АРМИРОВАННОГО ВОЛОКНОМ ЭЛАСТОМЕРНОГО ИЗОЛЯТОРА ДЛЯ ЖЕЛЕЗОБЕТОННОГО ЗДАНИЯ ПРИ ЗЕМЛЯТРЕСЕНИЯХ

*Ван-Тхует Нго*

Факультет гражданского строительства, Университет Туйлоя, г. Ханой, ВЬЕТНАМ

**Аннотация:** Эластомерные изоляторы, армированные фибровым волокном без сцепления (U-FREI), являются относительно новым типом многослойной изоляции, в которой в качестве армирующего используются вместо стальных листов используются слои волокна. Такой слой устраивается непосредственно между верхней и нижней опорными пластинами без какого-либо соединения по поверхности контакта. Большинство ранее выполненных исследований, посвященных U-FREI, были связаны с каменными конструкциями. В данной работе динамические характеристики железобетонного здания, опирающегося на квадратные изоляторы U-FREI, исследуются методом конечных элементов с использованием программного обеспечения SAP2000 при зарегистрированных в реальном времени колебаниях грунта, вызванных землетрясением. Для исследования выбрано 4-этажное железобетонное здание, построенное во Вьетнаме. Сравнение динамических откликов здания с изоляцией основания и соответствующего здания с фиксированным основанием проводится для оценки сейсмостойкости. Результаты расчета методом конечных элементов показывают, что пиковые значения ускорения перекрытий, межэтажные смещения, а также пиковое значение смещения основания здания с изоляцией ниже, чем у соответствующего здания с фиксированным основанием. Выявлено, что U-FREI эффективны для повышения сейсмостойкости малоэтажных и средне этажных зданий.

**Ключевые слова:** изоляция основания, эластомерный изолятор, армированный волокном, эффективная горизонтальная жесткость, эффективность здания с изоляцией основания, землетрясение

## 1. INTRODUCTION

Base isolation is an effective solution to reduce the vulnerability of a structure when earthquakes occur [1,2]. Normally base isolators are usually placed above the substructure and below the superstructure of the building. Base isolation can undergo large horizontal displacement from earthquakes due to the low horizontal stiffness of the isolators. Moreover, the large equivalent viscous damping of the isolators is dissipated the energy of earthquakes transmitted to the superstructure. Meanwhile, the vertical stiffness of the isolators has a large value to ensure that the isolators can undergo the weight of the construction and the vertical loads acting on the superstructure.

Most of the buildings used the base isolators in the world are often of high importance and high cost [3]. They often use conventional multi-layer elastomeric isolator such as natural rubber bearing (NRB), high-damping rubber bearing (HDRB), and lead rubber bearing (LRB). Over the past two decades, a new type of multi-layer elastomeric isolator as un-bonded fiber reinforced elastomeric isolator (U-FREI) is studied and developed. The U-FREI consists of alternating layers of rubber and fiber fabric as reinforcement. It is installed directly between the substructure and superstructure without any connection at the interfaces. Therefore, when the isolator is subjected to horizontal displacement, elastomer layers at top and bottom of the U-FREI will lose contact with the supports lead to “rollover deformation” [4]. The U-FREI is lighter, easier in manufacturing and installation than the conventional multi-layer elastomeric isolator. It is expected to replace the conventional multi-layer elastomeric isolator for seismic response control of low and mid-rise lifeline buildings in developing countries like Vietnam, Indonesia, India, etc.

Some studies for the U-FREI have been conducted in recent times. The vertical and horizontal behavior of the U-FREI under cyclic loading was investigated by both finite element (FE) analysis and experimental tests [5-15].

These studies were determined the mechanical properties of the U-FREIs with different sizes, including horizontal stiffness, vertical stiffness and damping factor. Analytical approaches were proposed to calculate the effective plan area in contact with the support surfaces and the effective horizontal stiffness of the U-FREI [16,17]. Some shake table tests of the base-isolated buildings supported on U-FREIs were carried out to ascertain its effectiveness in controlling seismic response [18-20]. A little effort to apply the U-FREIs for the residential buildings in developing countries was presented [2,21-25]. Most of these studies investigated the seismic effectiveness of the base-isolated masonry buildings supported on U-FREIs. Thus, the seismic performance of the U-FREIs supported to the base-isolated reinforced concrete (RC) buildings should be further studied.

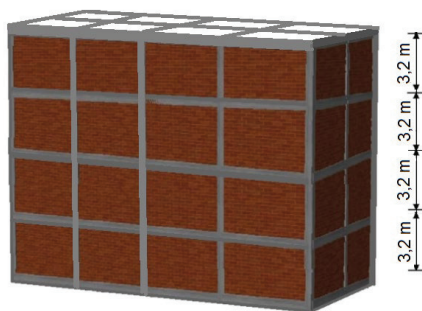
In this study, the seismic performance of a base-isolated RC building supported on square U-FREIs is investigated by FE analysis using SAP2000 software. A hypothetical base-isolated building constructed in Vietnam is selected for the study. The mechanical characteristics of the U-FREIs are determined with an analytical approach as proposed by the previous study. Dynamic response of the building under the action of various recorded real time history ground motions of earthquakes in two cases: fixed-base and base-isolated conditions are investigated. From results of FE analysis, comparison of the floor acceleration, inter-storey drift responses and base shear of the base-isolated building with those of the corresponding fixed-base building is carried out to evaluate the seismic vulnerability of the base-isolated building under earthquakes.

## 2. DESCRIPTION OF A BASE-ISOLATED RC BUILDING

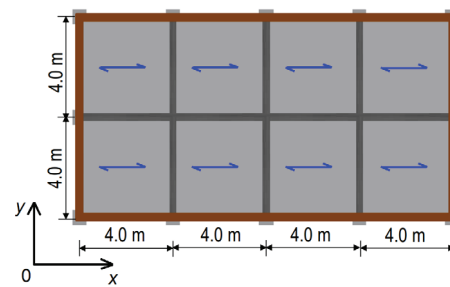
As mentioned above, U-FREI is a relatively new type of seismic isolator, which is expected to be used for low and mid-rise civil buildings.

There have not been many base-isolated buildings supported on the isolators. There is an actual base-isolated two-storey masonry building supported on square U-FREIs which was successfully constructed in October 2016 at Tawang, Arunachal Pradesh State, India. This is the first U-FREIs supported prototype low-rise building to be constructed anywhere in the world [2]. In this study, a hypothetical RC building supported on square U-FREIs is selected as the research object.

A base-isolated 4-storey RC building with hypothetical constructed location, hypothetical dimensions and hypothetical material properties is considered for this study. It is constructed in Muong Lay town, Dien Bien province, Vietnam. Dien Bien is a province in the north-western region, where has the largest seismic activity in Vietnam. Materials used in the building are concrete of B15 grade (weight per unit volume of  $25 \text{ kN/m}^3$ , modulus of elasticity of  $2.3 \times 10^7 \text{ kN/m}^2$  and poisson's ratio of 0.2) and reinforcement of CIII group grade ( $f_y = 400 \text{ N/mm}^2$ ) according to Vietnam design standard TCVN 5574 [26]. Cross-sectional dimensions of all beams and columns are  $0.30\text{m} \times 0.45\text{m}$  and  $0.30\text{m} \times 0.30\text{m}$  respectively. Thickness of all slabs is  $0.12\text{m}$ . There are 5 bays of  $4.0\text{m}$  in X-direction, 3 bays of  $4.0\text{m}$  in Y-direction, i.e. plan dimensions are  $16.0\text{m} \times 8.0\text{m}$ . Each floor height is  $3.2\text{m}$ . Brick masonry walls with thickness of  $0.11\text{m}$  are built around the perimeter of the building. Three-dimensional view and typical floor plan of the base-isolated building are shown in Fig. 1.



(a) View of the superstructure



(b) Typical floor plan

Figure 1. The base-isolated 4-storey RC building

The superstructure is placed on an isolation system consisting of fifteen square U-FREIs placed under fifteen columns (Fig. 2). There exists a rigid slab at the base level that connects all isolation elements. It is considered that the weight of the superstructure is equally transferred to each isolator under the column. The maximum possible vertical load on an isolator as computed considering all possible load combinations as per Vietnam standard TCVN 9386 (Design of structures for earthquake resistances) [27] is  $W = 580 \text{ kN}$ . The fixed-base period of the superstructure is estimated to be about 0.42 seconds (from simulated model in SAP2000 v.15.2.1 software [28]). The project site is located in Muong Lay town on a site with soil class B as per Vietnam standard [27].



Figure 2. View showing locations of base isolators in the building

### 3. SELECTING THE SIZE AND MECHANICAL CHARACTERISTICS OF SQUARE U-FREIS

#### 3.1. Methodology

##### 3.1.1. Shape factor

One of the most important parameters in the design of multi-layer elastomeric isolator is shape factor ( $S$ ) defined as the ratio of the

loaded area to load free area of a rubber layer [3]. For a square isolator with the width of  $a$  and a single rubber layer thickness of  $t_e$ , the shape factor is computed by

$$S = \frac{a}{4t_e} \quad (1)$$

Generally, for better seismic performance, the prototype isolators should have the value of shape factor more than 10 [3].

### 3.1.2. Horizontal stiffness of a square U-FREI

According to [3], the horizontal stiffness of a conventional multi-layer elastomeric isolator is given by

$$K_h^b = \frac{GA}{t_r} \quad (2)$$

where  $G$  is the initial shear modulus,  $A$  is the full cross-sectional area of the isolator (for a square isolator with the width of  $a$ , the full cross-sectional area is  $A = a^2$ ), and  $t_r$  is the total thickness of rubber layers in the isolator.

The horizontal stiffness of a U-FREI is calculated according to an analytical approach which is proposed by Ngo et al. [17] as

$$K_h^{ub} = \frac{G_{eff} A_{eff}}{t_r} \quad (3)$$

where  $G_{eff}$  is the effective shear modulus of isolator and  $A_{eff}$  is the effective plan area in contact with the support surfaces of the U-FREI at the horizontal displacement ( $u$ ).

The effective shear modulus ( $G_{eff}$ ) is affected by many factors such as the magnitude of the horizontal displacement ( $u$ ) and the value of the vertical load acting on the isolator. For a square isolator with the width of  $a$ , the effective shear modulus ( $G_{eff}$ ) is given as:

For  $0 < u \leq 1.0t_r$ :

$$G_{eff} = G \left[ 1 - \left( \frac{p_z}{p_{crit,0} \left( 1 - \left( \frac{u}{a} \right)^2 \right)} \right)^2 \right] \left( 1 - \frac{u}{a} \right) \quad (4)$$

For  $1.0t_r < u \leq 1.5t_r$ :

$$G_{eff} = G \left[ 1 - \left( \frac{p_z}{p_{crit,0} \left( 1 - \left( \frac{t_r}{a} \right)^2 \right)} \right)^2 \right] \left( 1 - \frac{t_r}{a} \right) \quad (5)$$

where  $p_{crit,0}$  is the critical stress state according to Kelly [29] and is given by

$$p_{crit,0} = \frac{P_{crit}}{a^2} \quad (6)$$

$$P_{crit} = \frac{\sqrt{2\pi GASr}}{t_r} \quad (7)$$

$$r = \frac{a}{2\sqrt{3}} \quad (8)$$

$r$  is the radius of gyration;  $p_z$  is the vertical pressure on the isolator and is calculated as

$$p_z = \frac{W}{A} \quad (9)$$

$W$  is the vertical load on the isolator.

According to [16], the effective plan area ( $A_{eff}$ ) of a square isolator with the width of  $a$  is calculated as

$$A_{eff} = a(a - d) \quad (10)$$

where,  $d$  is the projected length of the curved part of the rollover region along the horizontal plane as shown in Fig. 3, and is given as

$$d = \frac{25}{16} \alpha h \quad (11)$$



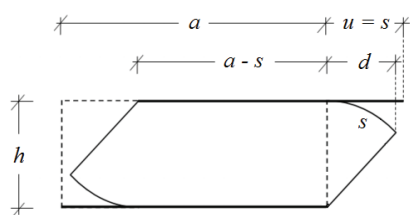


Figure 3. Deformed configuration of an U-FREI

where,  $h$  is the total height of the isolator,  $\alpha$  is a geometrical parameter which relates  $d$  and curved length ( $s$ ) at a given horizontal displacement ( $u$ ). The relation between  $u$ ,  $s$  and  $\alpha$  as proposed by Toopchi-Nezhad [16] is expressed as

$$u = s = \frac{25}{64} h \left[ 2\alpha\sqrt{1+4\alpha^2} + \ln\left(2\alpha + \sqrt{1+4\alpha^2}\right) \right] \quad (12)$$

Thus, for a known value of  $u$  and  $h$ ,  $\alpha$  is found from Eq. (12), which is used for the evaluation of  $A_{eff}$  using Eq. (10).

### 3.1.3. Vertical stiffness of a square U-FREI

Vertical stiffness ( $K_v$ ) of a multi-layer elastomeric isolator is given by [3]

$$K_v = \frac{E_c A}{t_r} \quad (13)$$

where  $E_c$  is the compression modulus of the isolator, for a square isolator is  $E_c = 6.73GS^2$ .

## 3.2. Selecting the size of square U-FREIs supported to the base-isolated building

A design procedure for determining the size of the conventional multi-layer elastomeric isolators (including NRBs, HDRBs, LRBs) supported to base-isolated structures was presented by Mayes and Naeim [30]. There are few documents giving detailed design procedure for determining the size of the U-FREIs. Ngo [31] was proposed a design procedure following the design provisions of ASCE 7 [32] for selecting the size of U-FREIs supported to a base-isolated building. In this study, the step-by-step selecting size of square U-FREIs is presented according to the design procedure proposed by Ngo [31].

**Step 1:** Evaluation of spectral response acceleration parameter at a period of 1 second,  $S_I$  ( $S_I \leq 0.60$ ):

According to Vietnam standard TCVN 9386 [27], the peak value of reference ground acceleration in Muong Lay town is  $a_{gR} = 0.1516g$ . Note that the spectral acceleration ( $S_I$ ) in ASCE 7 [32] is calculated according to the repetition period of  $T_{ASCE} = 2500$  years, while it, in the Vietnam standards, is calculated according to the repetition period of  $T_{VN} = 500$  years [27]. Therefore, it is necessary to convert the peak value of reference ground acceleration in Vietnam standards from the 500-year repetition period to the 2500-year repetition period. According to [27], the conversion formula is as follows:

$$S_I = (T_{VN} / T_{ASCE})^{(-1/3)} (a_{gR} / g) \quad (14)$$

$$S_I = (500 / 2500)^{(-1/3)} (0.1516g / g)$$

$$S_I = 1.71 \times 0.1516 = 0.2592$$

**Step 2:** Determine the site coefficient,  $F_v$ :

The building is located on a site with soil class B as per Vietnam standard [27]. The site soil class B in TCVN 9386 [27] corresponds to the site soil class C in ASCE 7 [32]. Thus, the value of  $F_v = 1.50$  is obtained from Table 11.4-2 in ASCE 7 [32] for site class C and  $S_I = 0.2592$ .

**Step 3:** Determine the seismic coefficient,  $S_{M1}$ :

The spectral coefficient needed for calculation of minimum displacements is obtained from Eq. (15):

$$S_{M1} = F_v S_I \quad (15)$$

$$S_{M1} = 1.50 \times 0.2592 = 0.389$$

**Step 4:** Select the damping coefficient,  $B_M$ :

The equivalent viscous damping of the U-FREIs is usually in the range of 6% to 15% [1-5]. For preliminary design purpose, 10% damping is assumed for isolator type of U-FREI. From Table Table 17.5-1 in ASCE 7 [32],  $B_M = 1.20$ .

**Step 5:** Select a desired period of the isolated structure at the design displacement,  $T_M$ :

The effective period of the base-isolated structure at the design displacement is calculated from Eq. (16):

$$T_M \geq 3T_{fixed-base} \quad (16)$$

where  $T_{fixed-base}$  is the fixed-base period of the building.  $T_M$  is often selected in range from 1.5 to 2.5 seconds for low and mid-rise civil buildings. Thus,

$$T_M \geq 3 \times 0.42 = 1.26(\text{sec})$$

Take  $T_M = 1.60$  (sec) for preliminary design.

**Step 6:** Estimate the effective horizontal of the isolator,  $K_h$ :

The effective horizontal stiffness of the isolator is obtained from Eq. (17) as

$$T_M = 2\pi \sqrt{\frac{W}{K_{M,min}g}} \rightarrow K_h = \frac{W}{g} \left( \frac{2\pi}{T_M} \right)^2 \quad (17)$$

where  $K_{M,min}$  is the minimum effective horizontal stiffness of the isolator at the design displacement ( $T_M$ ),  $W$  is the maximum possible vertical load on an isolator ( $W = 580$  kN) and  $g$  is the acceleration of gravity ( $g = 9.81$  m/s<sup>2</sup>). Thus,

$$K_h = \frac{580}{9.81} \times \left( \frac{2\pi}{1.60} \right)^2 = 911.8(\text{kN} / \text{m})$$

**Step 7:** Estimate the design horizontal displacement,  $D_M$ :

The design displacement is obtained from Eq. (18) as

$$D_M = \left( \frac{g}{4\pi^2} \right) \frac{S_M T_M}{B_M} \quad (18)$$

$$D_M = \left( \frac{9.81}{4\pi^2} \right) \times \frac{0.389 \times 1.60}{1.20} = 0.129(\text{m})$$

**Step 8:** Estimate the total rubber thickness required,  $t_r$ :

$$\gamma = \frac{D_M}{t_r} = 150\% \rightarrow t_r = \frac{D_M}{1.5} \quad (19)$$

$$t_r = \frac{0.129}{1.50} = 0.086(\text{m}) = 86(\text{mm})$$

**Step 9:** Choose the full cross-sectional area of the U-FREI:

$$A > \frac{K_h t_r}{G} \quad (20)$$

The initial shear modulus ( $G$ ) depends on the type or rubber used in the isolator. Generally, the value of  $G$  is selected in range from 0.5 to 1.35 MPa. To take a typical rubber with  $G = 0.90$  MPa. From Eq. (20):

$$A > \frac{911.8 \times 0.086}{0.9 \times 10^3} = 0.0871(\text{m}^2)$$

$$a > \sqrt{A} = \sqrt{0.0871} = 0.295(\text{m})$$

In fact, the horizontal stiffness of a U-FREI is calculated by Eq. (3) relates to the reduction in shear modulus with increasing displacement and the effective plan area in contact with the support surfaces [17]. Thus, it is chosen  $a = 0.32$  (m) = 320 (mm) for the square U-FREIs supported to the base-isolated building.

**Step 10:** Choose the number of rubber layers,  $n_e$ , thickness of a rubber and fiber layer,  $t_e$  and  $t_f$ , and total thickness of U-FREI,  $h$ :

According to [3], the shape factor typical for seismic isolation is in range of 10 to 20. Selecting a shape factor of  $S = 16$  for the isolators of seismic isolation, from Eq. (1) we can calculate the thickness of an individual rubber layer,  $t_e$ , as

$$t_e = \frac{a}{4S} = \frac{320}{4 \times 16} = 5(\text{mm})$$

Choose  $t_e = 5$  (mm). Thus, the number of rubber layers is  $n = 86/5 = 17.2$ . Choose  $n = 18$ .

The total thickness of rubber layers in the isolator is

$$t_r = n \times t_e = 18 \times 5 = 90(\text{mm})$$

Using  $t_f = 0.55$  (mm) thick of a carbon fiber reinforcement layer. The total height of the isolator is

$$h = 90 + 0.55 \times (18 - 1) = 99.35 \approx 100 \text{ (mm)}$$

Thus, the sizes of the isolators are **320x320x100** (mm). Three-dimensional view of the U-FREI is shown in Fig. 4.



Figure 4. View showing sizes of the U-FREIs

### 3.3. Determination of mechanical characteristics of the square U-FREIs

#### 3.3.1. The shape factor

The actual shape factor of the U-FREIs is:

$$S = \frac{a}{4t_e} = \frac{320}{4 \times 5} = 16$$

#### 3.3.2. The effective horizontal stiffness ( $K_h^{ub}$ )

According to [32], the limit horizontal displacement amplitude of an isolation system is  $1.50t_r$  (135 mm). Therefore, values of the effective horizontal stiffness of the U-FREIs at the increasing horizontal displacement amplitude up to  $1.50t_r$  are determined with the analytical approach above, and are given results in Table 1.

According to [32], the effective horizontal stiffness of an isolator relates the shear force and the horizontal displacement amplitude by

$$K_h = \frac{F}{u} \tag{21}$$

From Eq. (21), the shear force of the isolator is obtained by

$$F = K_h u \tag{22}$$

Table 1. Effective horizontal stiffness of the U-FREIs

$u$ (mm)	$u/t_r$	$G_{eff}$ (N/mm <sup>2</sup> )	$\alpha$	$d$ (mm)	$A_{eff}$ (mm <sup>2</sup> )	$K_h^{ub}$ (kN/m)
20.0	0.22	0.8374	0.1267	19.80	96065.00	838.86
40.0	0.44	0.7815	0.2464	38.50	90080.00	734.03
60.0	0.67	0.7254	0.3559	55.61	84605.00	639.97
80.0	0.89	0.6721	0.4505	70.39	79875.00	559.79
90.0	1.00	0.6412	0.5015	78.36	77325.00	517.00
112.5	1.25	0.6412	0.5983	93.48	72485.00	484.64
135.0	1.50	0.6412	0.6867	107.30	68065.00	455.09

The shear force-horizontal displacement amplitude relationships of these isolators with increasing horizontal displacement amplitude up to  $1.50t_r$  as obtained from the analytical approach and idealized lines as given by bi-linear behaviour are shown in Fig. 5. The bi-linear behaviour is selected because this model can be effectively used for all isolation systems used in practice.

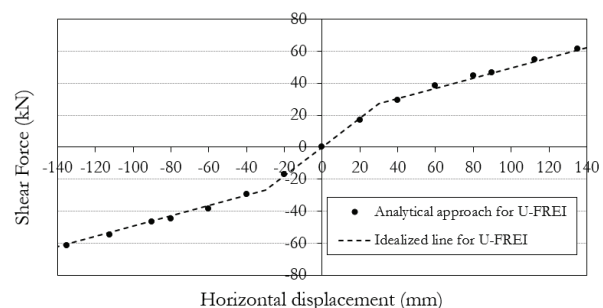


Figure 5. Shear force – horizontal displacement amplitude relationships of the isolators

### 3.3.3. The Vertical Stiffness of U-FREIs

The compression modulus and vertical stiffness of the U-FREIs are calculated as

$$E_c = 6.73 \times 0.90 \times 16^2 = 1550.59 \text{ (N/mm}^2\text{)};$$

$$K_v = \frac{1550.59 \times 320^2}{90} = 1764229.12 \text{ (kN/m)}.$$

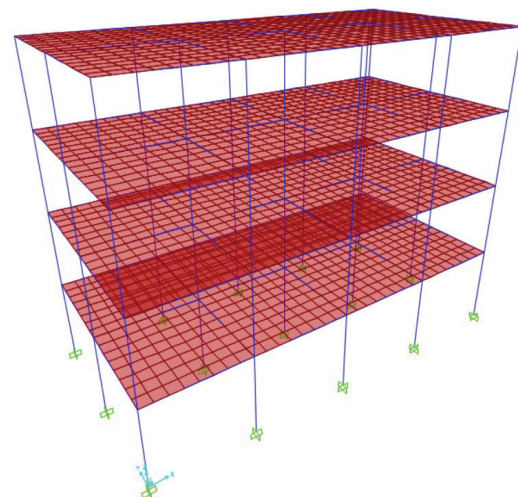
## 4. INVESTIGATION OF THE EFFECTIVENESS OF THE BASE-ISOLATED BUILDING UNDER EARTHQUAKES

The response of the base-isolated building supported on the U-FREIs and the corresponding fixed-base building under the action of various recorded real time-history ground motions of earthquakes are investigated by FE analysis using SAP2000 v.15.2.1 software [28]. Comparison of the floor acceleration, inter-storey drift responses and base shear of the base-isolated building with those of the corresponding fixed-base building is carried out to evaluate the seismic vulnerability of the base-isolated building under earthquakes.

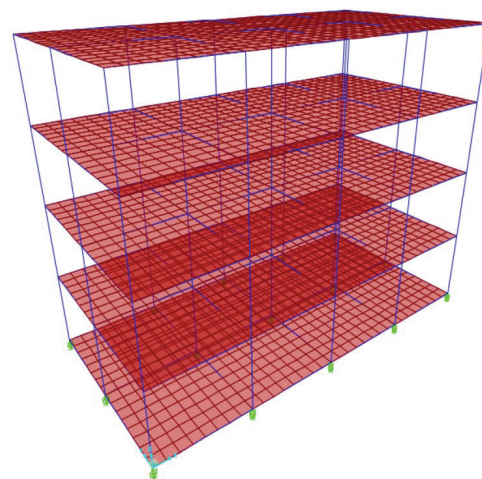
The fixed-base and base-isolated buildings are simulated in 3D finite element model by SAP2000 (Fig. 6). The beams and columns are modelled using frame elements. All floors are modelled using shell elements, in which each floor is assigned by a diaphragm constraint. For the base-isolated building, U-FREIs are modelled by rubber isolator element defined under link type of elements (rubber isolator). The nonlinear force-horizontal displacement behaviour (bi-linear curve) of the isolators as shown in Fig. 5 is used to represent the mechanical properties of the isolators along X and Y-axis. The vertical stiffness of the isolators above is used to present the mechanical properties of the isolators along Z-axis. For the fixed-base building, all nodes at ground level are fixed in all the directions.

The dynamic responses of the fixed-base and base-isolated buildings under the action of

various recorded real earthquake time-history ground motions of earthquakes are investigated by time history analysis. Two time-history ground motions from real earthquake records as El-Centro earthquake (USA, 18/05/1940, Comp – 180, peak acceleration value of 0.32g) and Kobe earthquake (Japan, 16/01/1995, Comp – FUK000, peak acceleration value of 0.33g) as shown in Fig. 7, are selected to investigate the seismic performance of the base-isolated building. Time history analysis is carried out along the weaker axis of the building, i.e. Y-axis (Fig. 1b).



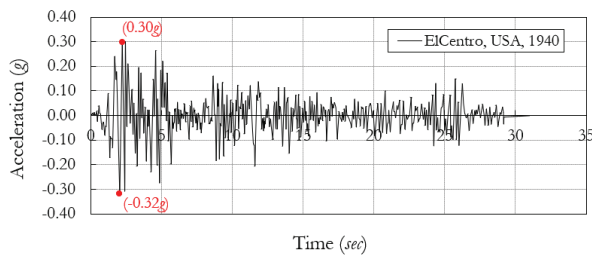
(a) Fixed-base building



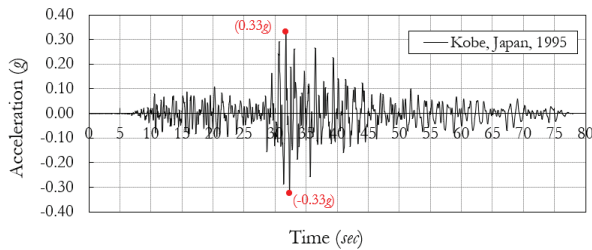
(b) Base-isolated building

Figure 6. Three-dimensional FE model of the building





(a) El-Centro earthquake



(b) Kobe earthquake

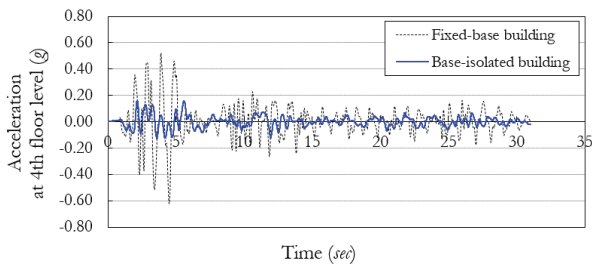
Figure 7. Real time-history record of selected earthquake motions

Comparison of the peak absolute values of floor accelerations, inter-storey drifts and base shear of the base-isolated building with those of the fixed-base building are presented in Table 2. Comparison of the detailed time-history of floor acceleration at roof level (the level has the maximum magnitude of peak floor acceleration), inter-storey drifts at the 2<sup>nd</sup> storey (the level has the maximum magnitude of peak inter-storey drift) and base shear of the base-isolated and fixed-base buildings under each earthquake excitation are shown in Figs. 8-10 respectively.

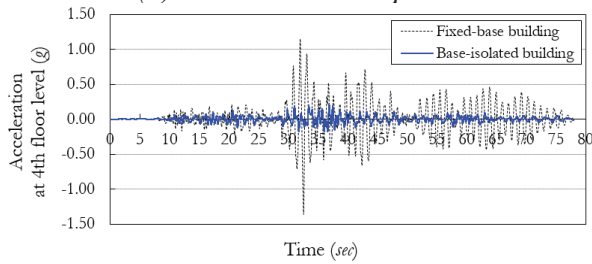
It may be observed from Table 2 that the magnitudes of peak floor acceleration and inter-storey drifts at different floor levels, and the magnitude of peak base shear of base-isolated building are lower than those of fixed-base building. For example, the peak floor acceleration value at roof level, the peak inter-storey drift value at 2<sup>nd</sup> storey and peak value of base shear of the base-isolated building are reduced by (74.2%, 72.6% and 69.9% respectively), (84.7%, 88.0% and 84.4% respectively) as compared to the corresponding values in the fixed-base building under El-Centro, Kobe earthquakes respectively. Further, the magnitudes of peak floor acceleration at different floor levels of the base-isolated building are almost the same under each excitation, while the magnitude of peak floor acceleration of the fixed-base building is amplified along the height of the building model. This finding is in agreement with the observation made by Das et al. [19] based on the shake table testing results of a scaled model of base-isolated un-reinforced brick masonry building supported on U-FREIs. It indicates that the possibility of any damage in the superstructure of the base-isolated building is clearly lower than that of fixed-base building. Thus, the mitigation of seismic vulnerability of the base-isolated building supported on the U-FREIs is better than that of the fixed-base building under the same earthquakes.

Table 2. Comparison of the peak values of dynamic responses of the fixed-base and base-isolated buildings under earthquakes

Parameter	Fixed-base building		Base-isolated building	
	El-Centro	Kobe	El-Centro	Kobe
Peak floor acceleration value at 1 <sup>st</sup> floor level (g)	0.35	0.55	0.12	0.14
Peak floor acceleration value at 2 <sup>nd</sup> floor level (g)	0.42	0.84	0.09	0.13
Peak floor acceleration value at 3 <sup>rd</sup> floor level (g)	0.46	1.11	0.13	0.14
Peak floor acceleration value at roof level (g)	0.62	1.37	0.16	0.21
Peak inter-storey drift value at 1 <sup>st</sup> storey (mm)	42.2	100.1	12.9	14.1
Peak inter-storey drift value at 2 <sup>nd</sup> storey (mm)	46.4	112.2	12.7	13.5
Peak inter-storey drift value at 3 <sup>rd</sup> storey (mm)	38.2	86.6	9.8	11.4
Peak inter-storey drift value at 4 <sup>th</sup> storey (mm)	20.8	45.9	5.2	6.5
Peak value of base shear (kN)	2788.9	6566.7	838.9	1023.1

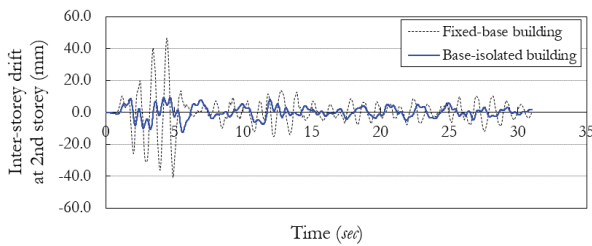


(a) El-Centro earthquake

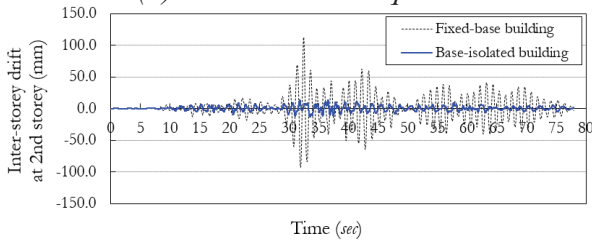


(b) Kobe earthquake

Figure 8. Floor acceleration responses at the roof level of the building under various earthquakes

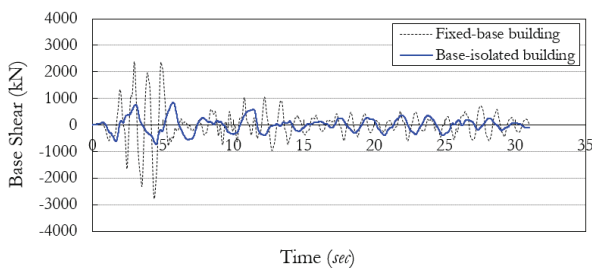


(a) El-Centro earthquake

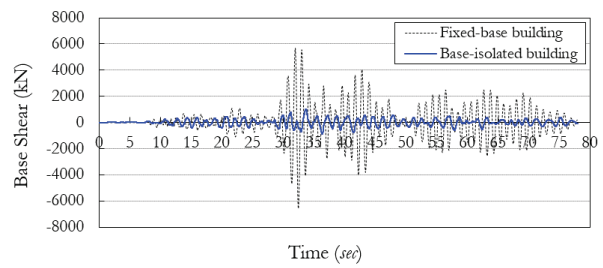


(b) Kobe earthquake

Figure 9. Inter-storey drift responses at the 2nd storey of the building under various earthquakes



(a) El-Centro earthquake



(b) Kobe earthquake

Figure 10. Base shear responses of the building under various earthquakes

## 5. CONCLUSION

This study presents the seismic performance of a base-isolated reinforced concrete building supported on square un-bonded fiber reinforced elastomeric isolators. A hypothetical base-isolated 4-storey RC building constructed in Muong Lay town, Dien Bien province, Vietnam is considered for the study. The size of the square U-FREIs is selected following the design provisions of ASCE 7. The mechanical properties of the square U-FREIs with the selected size, including horizontal and vertical stiffnesses, are calculated with an analytical approach as proposed by previous study. Investigation the time-history responses of both fixed-base and base-isolated buildings under the action of various recorded real earthquake time-history ground motions of earthquakes are carried out by FE analysis using SAP2000 software. From results of FE analysis, comparison of the dynamic responses of the fixed-base and base-isolated buildings is presented to evaluate the seismic vulnerability of the base-isolated building under earthquakes. The concluding remarks are as follows:

- Magnitudes of peak floor acceleration and inter-storey drifts at different floor levels of the base-isolated building are lower than those of the fixed-base building. Thus, the possibility of any damage in the superstructure of the base-isolated building is clearly lower than that of the corresponding fixed-base building.

- Magnitude of peak base shear of the base-isolated building is lower than that of the fixed-base building. The seismic vulnerability of the base-isolated building is mitigated in comparison with that of the corresponding fixed-base building under the same earthquakes.
- U-FREIs are found to be very effective in reducing seismic vulnerability of low and mid-rise RC buildings. Thus, U-FREIs are recommended for seismic isolation of low and mid-rise RC buildings.

## REFERENCES

1. **Kumar P., Petwal S.** (2019). Seismic performance of secondary systems housed in isolated and non-isolated building. *Earthquakes and Structures, an international journal*, 16(4), 401-413.
2. **Ngo V.T., Deb S.K., Dutta A.** (2018). Mitigation of seismic vulnerability of a prototype low-rise masonry building using U-FREIs. *Journal of Performance of Constructed Facilities, ASCE*, 32(2), 04017136.
3. **Naeim F., Kelly J.M.** (1999). Design of seismic isolated structures: From theory to practice. *John Wiley & Sons Inc.*, New York, USA.
4. **Toopchi-Nezhad H., Tait M.J., Drysdale R.G.** (2008). Lateral response evaluation of fiber-reinforced neoprene seismic isolator utilized in an unbonded application. *Journal of Structural Engineering, ASCE*, 134(10), 1627-1637.
5. **Moon B.Y., Kang G.J., Kang B.S., Kelly J.M.** (2002). Design and manufacturing of fiber reinforced elastomeric isolation. *Journal of Material Processing Technology*, 130-131, 145-150.
6. **Ashkezari G.D., Aghakouchak A.A., Kokabi M.** (2008). Design, manufacturing and evaluation of the performance of steel like fiber reinforced elastomeric seismic isolators. *Journal of Material Processing Technology*, 197, 140-150.
7. **Toopchi-Nezhad H., Tait M.J., Drysdale R.G.** (2009). Simplified analysis of a low-rise building seismically isolated with stable un-bonded fiber reinforced elastomeric isolators. *Canadian Journal of Civil Engineering*, 36(7), 1182-1194.
8. **Russo G., Pauletta M.** (2013). Sliding instability of fiber-reinforced elastomeric isolators in un-bonded applications. *Engineering Structures*, 48, 70-80.
9. **Spizzuoco M., Calabrese A., Serino G.** (2014). Innovative low-cost recycled rubber-fiber reinforced isolator: Experimental test and finite element analyses. *Engineering Structures*, 76, 99-111.
10. **Naghshineh A.K., Akyuz U., Caner A.** (2014). Comparison of fundamental properties of new types of fiber-mesh-reinforced seismic isolators with conventional isolators. *Earthquake Engineering and Structural Dynamics*, 43(2), 301-316.
11. **Dezfuli F.H., Alam M.S.** (2014). Performance of carbon fiber-reinforced elastomeric isolators manufactured in a simplified process: Experimental investigations. *Structural Control and Health Monitoring*, 21(11), 1347-1359.
12. **Osgooei P.M., Tait M.J., Konstantinidis D.** (2014). Finite element analysis of unbonded square fiber-reinforced elastomeric isolators (FREIs) under lateral loading in different directions. *Composite Structures*, 113, 164-173.
13. **Van Engelen N.C., Osgooei P.M., Tait M.J., Konstantinidis D.** (2014). Experimental and finite element study on the compression properties of modified rectangular fiber-reinforced elastomeric isolators (MR-FREIs). *Engineering Structures*, 74, 52-64.
14. **Ngo V.T.** (2020). Effect of shape factor on the horizontal response of prototype unbonded fiber reinforced elastomeric

- isolators under cyclic loading. *Structural Integrity and Life*, 20(3), 303-312.
15. **Ngo V.T.** (2021). Influence of vertical load on the horizontal response of prototype unbonded fiber reinforced elastomeric isolator. *Structural Integrity and Life*, 21(3), 229-237.
  16. **Toopchi-Nezhad H.** (2014). Horizontal stiffness solutions for unbonded fiber reinforced elastomeric bearings. *Structural Engineering and Mechanics, an international journal*, 49(3), 395-410.
  17. **Ngo V.T., Dutta A., Deb S.K.** (2017). Evaluation of horizontal stiffness of fibre reinforced elastomeric isolators. *Earthquake Engineering and Structural Dynamics*, 46(11), 1747-1767.
  18. **Toopchi-Nezhad H., Tait M.J., Drysdale R.G.** (2009). Shake table study on an ordinary low-rise building seismically isolated with SU-FREIs (stable unbonded-fiber reinforced elastomeric isolators). *Earthquake Engineering and Structural Dynamics*, 38(11), 1335-1357.
  19. **Das A., Deb S.K., Dutta A.** (2016). Shake table testing of un-reinforced brick masonry building test model isolated by U-FREI. *Earthquake Engineering and Structural Dynamics*, 45(2), 253-272.
  20. **Losanno D., Spizzuoco M., A. Calabrese A.** (2019). Bidirectional shaking table tests of unbonded recycled rubber fiber-reinforced bearings (RR-FRBs). *Structural Control and Health Monitoring*, 26(9), e2386.
  21. **Calabrese A., Losanno D., Spizzuoco M., Strano S., Terzo M.** (2019). Recycled rubber fiber-reinforced bearings (RR-FRBs) as base isolators for residential buildings in developing countries: The demonstration building of Pasir Badak, Indonesia. *Engineering Structures*, 192, 126-144.
  22. **Habieb A.B., Valente M., Milani G.** (2019). Base seismic isolation of a historical masonry church using fiber reinforced elastomeric isolators. *Soil Dynamics and Earthquake Engineering*, 120, 127-145.
  23. **Ngo V.T.** (2021). Effectiveness of base-isolated low-rise masonry building under excitation from earthquakes. *Magazine of Civil Engineering*, 108(8), 10803.
  24. **Habieb A.B., Formisano A., Milani G., Pianese G.** (2022). Seismic performance of Unbonded Fiber-Reinforced Elastomeric Isolators (UFREI) made by recycled rubber. Influence of suboptimal crosslinking. *Engineering Structures*, 256, 114038.
  25. **Losanno D., Ravichandran N., Parisi F.** (2023). Seismic fragility models for base-isolated unreinforced masonry buildings with fibre-reinforced elastomeric isolators. *Earthquake Engineering and Structural Dynamics*, 52( 2), 308-334.
  26. **TCVN 5574.** (2018). Concrete and reinforced concrete structures. *Vietnam Design standard*, Hanoi, Vietnam.
  27. **TCVN 9386.** (2012). Design of structures for earthquake resistances. *Vietnam standard*, Hanoi, Vietnam.
  28. **SAP2000 v.15.2.1.** (2014). CSI Analysis Reference Manual. *Computers and structures Inc.*, Berkeley, California, USA.
  29. **Kelly J.M.** (2003). Tension buckling multilayer elastomeric bearings. *Journal of Engineering Mechanics, ASCE*, 129(12), 1363-1368.
  30. **Mayes R.L., Naeim F.** (2001). Design of Structures with Seismic Isolation. in *The Seismic Design Handbook*, Springer, Boston, Massachusetts, USA, Ch. 14, 723-756.
  31. **Ngo V.T.** (2017). Seismic performance evaluation of prototype unbonded fibre-reinforced elastomeric isolators. PhD thesis, Department of Civil Engineering, Indian Institute of Technology Guwahati-781039, Assam, India.
  32. **ASCE 7.** (2016). Minimum design load for buildings and other structure. *American Society of Civil Engineers (ASCE)*, Reston, Virginia, USA.



## СПИСОК ЛИТЕРАТУРЫ

1. **Kumar P., Petwal S.** (2019). Seismic performance of secondary systems housed in isolated and non-isolated building. *Earthquakes and Structures, an international journal*, 16(4), 401-413.
2. **Ngo V.T., Deb S.K., Dutta A.** (2018). Mitigation of seismic vulnerability of a prototype low-rise masonry building using U-FREIs. *Journal of Performance of Constructed Facilities, ASCE*, 32(2), 04017136.
3. **Naeim F., Kelly J.M.** (1999). Design of seismic isolated structures: From theory to practice. *John Wiley & Sons Inc.*, New York, USA.
4. **Toopchi-Nezhad H., Tait M.J., Drysdale R.G.** (2008). Lateral response evaluation of fiber-reinforced neoprene seismic isolator utilized in an unbonded application. *Journal of Structural Engineering, ASCE*, 134(10), 1627-1637.
5. **Moon B.Y., Kang G.J., Kang B.S., Kelly J.M.** (2002). Design and manufacturing of fiber reinforced elastomeric isolation. *Journal of Material Processing Technology*, 130-131, 145-150.
6. **Ashkezari G.D., Aghakouchak A.A., Kokabi M.** (2008). Design, manufacturing and evaluation of the performance of steel like fiber reinforced elastomeric seismic isolators. *Journal of Material Processing Technology*, 197, 140-150.
7. **Toopchi-Nezhad H., Tait M.J., Drysdale R.G.** (2009). Simplified analysis of a low-rise building seismically isolated with stable un-bonded fiber reinforced elastomeric isolators. *Canadian Journal of Civil Engineering*, 36(7), 1182-1194.
8. **Russo G., Pauletta M.** (2013). Sliding instability of fiber-reinforced elastomeric isolators in un-bonded applications. *Engineering Structures*, 48, 70-80.
9. **Spizzuoco M., Calabrese A., Serino G.** (2014). Innovative low-cost recycled rubber-fiber reinforced isolator: Experimental test and finite element analyses. *Engineering Structures*, 76, 99-111.
10. **Naghshineh A.K., Akyuz U., Caner A.** (2014). Comparison of fundamental properties of new types of fiber-mesh-reinforced seismic isolators with conventional isolators. *Earthquake Engineering and Structural Dynamics*, 43(2), 301-316.
11. **Dezfuli F.H., Alam M.S.** (2014). Performance of carbon fiber-reinforced elastomeric isolators manufactured in a simplified process: Experimental investigations. *Structural Control and Health Monitoring*, 21(11), 1347-1359.
12. **Osgooei P.M., Tait M.J., Konstantinidis D.** (2014). Finite element analysis of unbonded square fiber-reinforced elastomeric isolators (FREIs) under lateral loading in different directions. *Composite Structures*, 113, 164-173.
13. **Van Engelen N.C., Osgooei P.M., Tait M.J., Konstantinidis D.** (2014). Experimental and finite element study on the compression properties of modified rectangular fiber-reinforced elastomeric isolators (MR-FREIs). *Engineering Structures*, 74, 52-64.
14. **Ngo V.T.** (2020). Effect of shape factor on the horizontal response of prototype unbonded fiber reinforced elastomeric isolators under cyclic loading. *Structural Integrity and Life*, 20(3), 303-312.
15. **Ngo V.T.** (2021). Influence of vertical load on the horizontal response of prototype unbonded fiber reinforced elastomeric isolator. *Structural Integrity and Life*, 21(3), 229-237.
16. **Toopchi-Nezhad H.** (2014). Horizontal stiffness solutions for unbonded fiber reinforced elastomeric bearings. *Structural Engineering and Mechanics, an international journal*, 49(3), 395-410.
17. **Ngo V.T., Dutta A., Deb S.K.** (2017). Evaluation of horizontal stiffness of fibre reinforced elastomeric isolators.

- Earthquake Engineering and Structural Dynamics*, 46(11), 1747-1767.
18. **Toopchi-Nezhad H., Tait M.J., Drysdale R.G.** (2009). Shake table study on an ordinary low-rise building seismically isolated with SU-FREIs (stable unbonded-fiber reinforced elastomeric isolators). *Earthquake Engineering and Structural Dynamics*, 38(11), 1335-1357.
  19. **Das A., Deb S.K., Dutta A.** (2016). Shake table testing of un-reinforced brick masonry building test model isolated by U-FREI. *Earthquake Engineering and Structural Dynamics*, 45(2), 253-272.
  20. **Losanno D., Spizzuoco M., A. Calabrese A.** (2019). Bidirectional shaking table tests of unbonded recycled rubber fiber-reinforced bearings (RR-FRBs). *Structural Control and Health Monitoring*, 26(9), e2386.
  21. **Calabrese A., Losanno D., Spizzuoco M., Strano S., Terzo M.** (2019). Recycled rubber fiber-reinforced bearings (RR-FRBs) as base isolators for residential buildings in developing countries: The demonstration building of Pasir Badak, Indonesia. *Engineering Structures*, 192, 126-144.
  22. **Habieb A.B., Valente M., Milani G.** (2019). Base seismic isolation of a historical masonry church using fiber reinforced elastomeric isolators. *Soil Dynamics and Earthquake Engineering*, 120, 127-145.
  23. **Ngo V.T.** (2021). Effectiveness of base-isolated low-rise masonry building under excitation from earthquakes. *Magazine of Civil Engineering*, 108(8), 10803.
  24. **Habieb A.B., Formisano A., Milani G., Pianese G.** (2022). Seismic performance of Unbonded Fiber-Reinforced Elastomeric Isolators (UFREI) made by recycled rubber. Influence of suboptimal crosslinking. *Engineering Structures*, 256, 114038.
  25. **Losanno D., Ravichandran N., Parisi F.** (2023). Seismic fragility models for base-isolated unreinforced masonry buildings with fibre-reinforced elastomeric isolators. *Earthquake Engineering and Structural Dynamics*, 52( 2), 308-334.
  26. **TCVN 5574.** (2018). Concrete and reinforced concrete structures. *Vietnam Design standard*, Hanoi, Vietnam.
  27. **TCVN 9386.** (2012). Design of structures for earthquake resistances. *Vietnam standard*, Hanoi, Vietnam.
  28. **SAP2000 v.15.2.1.** (2014). CSI Analysis Reference Manual. *Computers and structures Inc.*, Berkeley, California, USA.
  29. **Kelly J.M.** (2003). Tension buckling multilayer elastomeric bearings. *Journal of Engineering Mechanics, ASCE*, 129(12), 1363-1368.
  30. **Mayes R.L., Naeim F.** (2001). Design of Structures with Seismic Isolation. in *The Seismic Design Handbook, Springer*, Boston, Massachusetts, USA, Ch. 14, 723-756.
  31. **Ngo V.T.** (2017). Seismic performance evaluation of prototype unbonded fibre-reinforced elastomeric isolators. PhD thesis, Department of Civil Engineering, Indian Institute of Technology Guwahati-781039, Assam, India.
  32. **ASCE 7.** (2016). Minimum design load for buildings and other structure. *American Society of Civil Engineers (ASCE)*, Reston, Virginia, USA.

---

*Van-Thuyet Ngo*, Civil Engineering Department, Thuyloi University, Hanoi, Vietnam. E-mail: thuyet.kcct@tlu.edu.vn

*Ван-Тхует Нго*, Факультет гражданского строительства, Университет Гуйлоя, Ханой, Вьетнам. E-mail: thuyet.kcct@tlu.edu.vn